INSTITUTE OF PHYSICS PUBLISHING MODELLING AND SIMULATION IN MATERIALS SCIENCE AND ENGINEERING

Modelling Simul. Mater. Sci. Eng. **11** (2003) 487–501 PII: S0965-0393(03)63234-1

A Concurrent multiscale finite difference time domain/molecular dynamics method for bridging an elastic continuum to an atomic system

Krishna Muralidharan, P A Deymier and J H Simmons

Department of Materials Science and Engineering, The University of Arizona, Tucson, AZ 85721, USA

Received 16 September 2002, in final form 4 May 2003
Published 6 June 2003
Online at stacks.iop.org/MSMSE/11/487

Abstract

A multiscale methodology that couples a finite difference time domain (FDTD) system (representing an elastic continuum) and an atomistic molecular dynamics (MD) system is proposed. The handshaking involves a parallel coupling of both the length and timescale. The FDTD–MD 'interface' is probed by a wave packet and the elastic impedance mismatch between the two systems is studied by examining the part of the probing wave packet that gets reflected from the interface. The reflected part is characterized in both temporal and frequency domains. Results show that only a small part of the wave is reflected from the interface, indicating a near seamless bridging of the two systems. Further, thermalization of the MD region results in transmission of additional energy into the FDTD region, with the transmitted energy corresponding to frequencies much higher than the central frequency of the probing wave packet. A characteristic resonant frequency exists between the MD and the FDTD regions, which is a result of a feedback between the two regions.

1. Introduction

Multiscaling has recently received much attention in several branches of physical sciences. In materials, a large part of the work is devoted to modern simulation methods involving coupling of length scales and sometimes timescales; they can be characterized as serial or concurrent. In serial methods a set of calculations at a fundamental level (small length scale) is used to evaluate parameters for use in a more phenomenological model that describes a phenomenon of interest at longer length scales. For example, atomistic simulations can be used to obtain the constitutive behaviour of finite elements (FEs), which are then used to simulate larger scale problems [1]. Several research groups are presently working productively on such methods, and several applications can be found [2, 3].

Concurrent methods rely on coupling seamlessly different computational methodologies applied to different regions of the material. For example, crack propagation is a problem that was tackled early on by multiscale methods [1, 4]. Atomic simulation techniques (molecular dynamics (MD)) were used to model the crack tip where large deformations (even bond breakage) occur and continuum approaches (FE methods) were used to model the region far away from the crack tip. Broughton and co-workers [5] proposed an algorithm involving handshaking between FEs, MD and semi-empirical tight-binding (TB) regions. This algorithm was able to dynamically track a crack propagating through silicon. The handshaking between the MD and FE regions was achieved by drawing an imaginary surface between them. Within the range of the MD interatomic potential from this surface, FE mesh points were located at equilibrium atomic sites. Moving away from this overlapping region into the FE region, the mesh spacing was made larger. Any FE that crosses the interface contributed half its weight to a conservative Hamiltonian. Similarly any MD interaction that crossed the interface also contributed half its weight. Kohlhoff *et al* [6] introduced a similar transition region between the atomic and continuous regions. They also scaled down the FE size to the atomic scale in this transition region. Unlike the work of Broughton *et al* the interface was of finite size and not sharp. Abraham *et al* [7] combined the above two techniques by constructing an explicit Hamiltonian for the atoms and the FE nodes in the transition region by weighing their contributions with respect to their distance away from the middle of the interface. Ogata and co-workers [8] used a similar algorithm to study chemical reactions and their interplay with mechanical phenomena in materials, such as in the oxidation of Si (111) surface. The quasicontinuum method formulated by Shenoy *et al* [9], links atomistic and continuum models through a reduction of the full set of atomistic degrees of freedom, to model crystals with more than one grain, grain boundary structures and their energetics. In this method, the total energy of the system is expressed as a weighted sum of contributions of representative atoms. The local environment of atoms is taken into account, and depending on the local deformation gradient, the atomic energies are calculated.

In linear elasticity the fundamental properties such as stress, strain, moduli are thermo-mechanical quantities. These quantities are defined such that they satisfy the thermodynamic and the long time limit. That is, these quantities represent averages over a large enough number of microscopic constituents and nearly infinite time. Calculating some of these quantities from atomistic models does not present significant difficulties as long as large enough systems and long enough times are used. This constitutes the basis for coarse graining that enables the extension of atomistic systems into the realm of continuous models with seamless coupling between length scales [10]. Problems in bridging continuum (e.g. FE) and atomistic regions may arise when the continuum or part of the continuum region is pushed outside the thermodynamic and long time limit. This is the case in many of the methodologies briefly reviewed above where the FE coupled to an MD region are reduced to 'atomic' dimensions. The spatial coupling between unphysically small FE and atoms implies also that the long time limit may not be satisfied. In addition, an elastic continuum does not obey the same physics over all possible wavelengths as that of a discrete atomic system. This physical mismatch is easily noted in the dispersion relations of both systems that overlap only in the long wavelength limit [11]. Based on the above observations, one can expect an elastic impedance mismatch between a continuum and atomic simulation when an attempt is made to couple them.

In this paper, we report on a study undertaken to examine and quantify the impedance mismatch between an elastic continuum and an atomistic region as the continuum spatial and temporal scales are forced toward atomic scales. We have coupled dynamically an elastic continuum modelled with the finite difference time domain (FDTD) method and an atomistic system modelled with MD. The impedance mismatch at the interface between the MD and

the FDTD systems is probed with an incoming elastic wave packet with broadband spectral characteristics centred on a predetermined central frequency. Reflection of part of the probe wave packet is a sign of impedance mismatch between the two systems. This reflection is characterized in the time and frequency domains over spatial and timescales ranging from atomic scales to the thermodynamic/long time limit scales.

This paper is organized as follows. In section 2 we briefly review the FDTD and MD method and pay particular attention to their coupling. Results and a discussion of the results are reported in section 3. Conclusions drawn from this study in terms of interfacing continuum and atomic regions are presented in section 4.

2. Methodology

Here we briefly review: in section 2.1, the FDTD method used to simulate the behaviour of an elastic continuum, in subsection 2.2, the atomistic method of MD. In subsection 2.3, we give a description of the system and its physical parameters. The approach used to couple the two methodologies is presented in some detail in subsection 2.4 with particular attention paid to the coupling in space and time. Finally, the probing wave packet is described in subsection 2.5.

2.1. FDTD method

The FDTD method solves numerically the elastic wave equation in homogeneous or inhomogeneous media. The elastic wave equations are integrated by means of discretization in both the spatial and the time domains [12, 13]. More specifically, real space is discretized into a grid on which all the variables and parameters are defined. The main variables are the acoustic displacement and the stress field at every site on the grid. The relevant parameters of the system are the densities and elastic constants for each constitutive element. The relevant parameters of the simulation are the grid spacing and the size of the time step. Appropriate boundary conditions such as periodic boundary conditions or absorbing boundary conditions are applied.

The FDTD scheme discretizes the wave equation $\partial^2 u_i/\partial t^2 = (1/\rho)(\partial T_{ij}/\partial x_j)$ in both the spatial and time domains and explicitly calculates the evolution of the displacement 'u' in the time domain. (T_{ij} is the stress tensor, ρ is the density, and u_n is the displacement of the nth element.) For the sake of simplicity, we limit the system to one-dimensional propagation. The FDTD region is discretized into N one-dimensional elements. We assume the FDTD region to be infinitely stiff in the other two directions. The elastic wave equations are approximated using centre differences in both time and space. The displacement u_n of any element 'n' at each time step is a function of the stress gradient $\sigma_n'(t)$ across that element. The displacement and the stress evolution of the system is given by

$$\begin{aligned}
\varepsilon_n(t+\Delta t) &= \frac{u_{n+1}(t) - u_n(t)}{\Delta x},\\
\sigma_n(t+\Delta t) &= C_{11n}\varepsilon_n(t+\Delta t),\\
\sigma_n'(t+\Delta t) &= \frac{\sigma_{n+1}(t+\Delta t) - \sigma_n(t+\Delta t)}{\Delta x},\\
u_n(t+\Delta t) &= 2u_n(t) - u_n(t-\Delta t) + \frac{\Delta t^2}{\rho_n(t)}[\sigma_n'(t)],
\end{aligned} \tag{1}$$

where Δx is the length of each element, Δt is the size of the FDTD time step, and ε_n, C_{11n}, and ρ_n are the strain, stiffness and the density of the nth element. Thus in this technique we can predict the displacement of every element knowing the stress on that element. We assume that

the stress on any element is uniform. Absorbing boundary conditions [11] are implemented in order to prevent reflection from the end elements of the FDTD mesh. The following relations denote the boundary conditions;

$$\begin{aligned} u_N(t+\Delta t) &= u_{N-1}(t) + \frac{c_o\Delta t - \Delta x}{c_o\Delta t + \Delta x} u_{N-1}(t+\Delta t) - u_N(t), \\ u_1(t+\Delta t) &= u_2(t) + \frac{c_o\Delta t - \Delta x}{c_o\Delta t + \Delta x} u_2(t+\Delta t) - u_1(t), \end{aligned} \tag{2}$$

where $c_o = \sqrt{C_{11}/\rho}$ and corresponds to the longitudinal velocity of the elastic wave through the medium.

2.2. MD method

The essence of MD methods involves solving the N-body problem of classical mechanics [14]. In other words, it involves solving Newton's equations of motion for a given set of particles, the interactions between particles governed by an interatomic potential, enabling one to keep track of the evolution of the system in phase space. The equations of motions are solved using standard finite difference schemes at each time step of the simulation. An MD simulation can be carried out under a variety of constant thermodynamic conditions. Here we use the macroscopic conditions of constant strain, number of molecules and temperature. In our studies, the MD system is propagated through phase space by solving for the equations of motion at each time step using the Verlet integrator. Temperature is maintained constant via a momentum rescaling procedure. Periodic boundary conditions are employed.

2.3. Model system

The elastic system to be probed is chosen to be argon. The elastic constant C_{11} was found from a series of MD simulations carried out under the following conditions: the model for the atomic system was a three-dimensional face centred cubic (FCC) crystal with periodic boundary conditions containing 500 particles interacting through a 6–12 Lennard-Jones potential with parameters chosen to simulate argon. The interatomic potential was truncated at a distance of 8.51 Å. The uniaxial long-time limit stress (σ)–strain (ε) curve for that crystal (figure 1) was obtained at 46 K with the temperature maintained via a velocity-rescaling scheme. For these calculations, a strain was applied in one direction while maintaining the length of the other edges of the simulation cell rigid. The strain was applied in increments of 2×10^{-4} in the interval [−0.1 to 0.1] and the resulting stress was then calculated from a virial-like equation [15] by averaging over 5000 MD time steps. An MD time step (dt) equals 10.0394 fs. The curve was then fitted to a third degree polynomial (equation (2)).

$$\sigma = 4.304 \times 10^{10}\varepsilon^3 - 1.54 \times 10^{10}\varepsilon^2 + 3.045 \times 10^9\varepsilon. \tag{3}$$

2.4. FDTD/MD coupling

An adaptive mesh and algorithm method (AMAR) developed by Garcia *et al* [16] involved embedding a direct simulation Monte Carlo (DSMC) particle method within a Navier–Stokes continuum method solver at the level of an adaptive mesh refinement (AMR) hierarchy. In AMAR, the DSMC region uses a time step that is comparable to that of the finest continuum grid. This is extremely useful for problems that span many timescales because a small time step is used in regions that require high resolution and this method has been successfully used to study the flow of a fluid past a sphere, and the compression of gases by a movable piston.

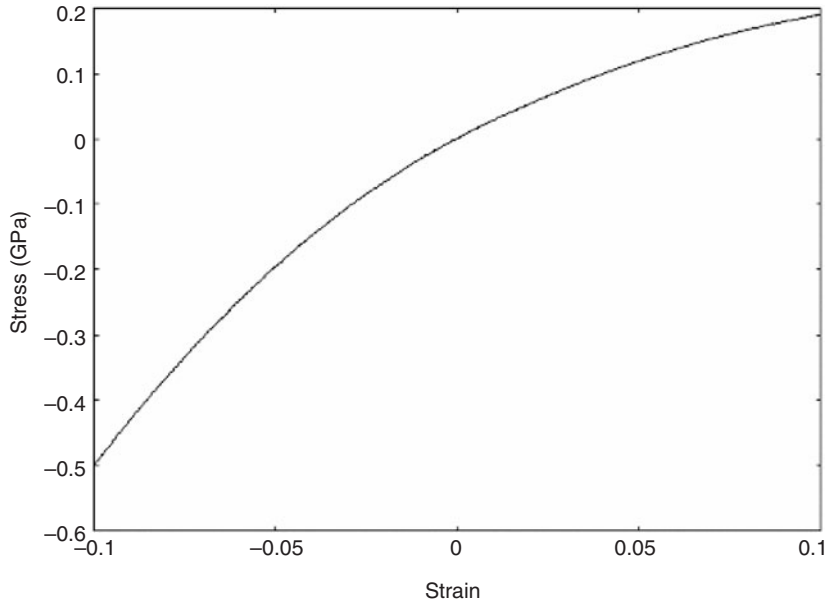

Figure 1. Uniaxial stress vs strain curve for the LJ–MD system.

The concept of using different time steps to address different length scales has been the idea behind the 'time scaling' involved in our simulations.

The handshaking is handled by replacing one FDTD element by a three-dimensional MD cell, the MD cell parameters chosen to exactly match the 'model MD system'. As shown in equations (1), the equations of motion for the propagation of the wave through the medium involves solving for the displacement as well as the stress fields for every FDTD element at every FDTD time step. The stress and the strain for every element are assumed to be uniform over its length. Thus, when an FDTD element is replaced by an MD cell, the equivalent displacement and stress for the element is calculated by uniaxially straining the MD cell along the direction of the wave propagation (the strain is obtained from equations (1)). The condition of rigidity in the other two directions is satisfied by keeping the length of the edges of the MD cell constant in these directions. The average value of the MD stress is evaluated for every FDTD time step with the final configuration of the MD atoms obtained at the previous FDTD time step serving as the initial state for the current MD calculation.

Since the continuum is assumed to be perfectly elastic, the elastic constant (C_{11}) of the FDTD region was chosen to be 3.045 GPa, which corresponds to the linear term of equation (2). This ensures a coarse serial coupling between the MD and FDTD region.

2.4.1. Time scaling. A preliminary study of the wave propagation characteristics indicated that the FDTD time step (Δt_{crit}) had to be smaller than ($\Delta x/2c_{\mathrm{o}}$) for a stable algorithm. At every FDTD time step, the MD stress is calculated by averaging over N_{md} ($=\Delta t/\mathrm{d}t$) time steps, with $\Delta t \leqslant \Delta t_{\mathrm{crit}}$. A reduction in Δt automatically leads to a decrease in the number of MD time steps over which stress is averaged (for every FDTD time step). It is therefore possible to push the time coupling between the two simulation techniques in such a way that one achieves in the smallest limit, a one to one correspondence between the two time steps. The FDTD/MD hybrid method, therefore, allows us to test a range of time

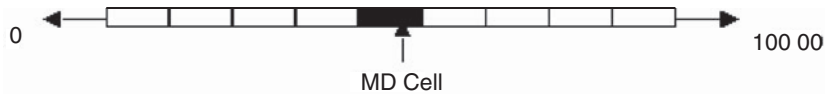

Figure 2. An illustrative representation of the system consisting of 10 000 elements; the open boxes represent FDTD elements and the darkened box corresponds to the MD cell.

scaling conditions from coarse graining to time matching between a continuum and an atomic system.

2.4.2. Spatial coupling. The number of FDTD elements is chosen to be 10 000. The length of each FDTD element (Δx) was chosen to equal the zero pressure box length of the MD cell (26.67 Å). The central wavelength of the wave packet was chosen to be an integral multiple of Δx, to ensure stability of the FDTD algorithm.

2.5. Probing signal

The probing wave packet is a one-dimensional wave packet and is of the form $a_0 \cos(-kx) \exp(-(kx)^2/2)$, where k is the wave vector, and a_0 the maximum amplitude of the wave. The wave is propagated through the medium with an initial longitudinal velocity c_0. The signal's frequency spectrum is broadband and the central frequency of the wave packet ν equals $c_0 k$.

3. Results

3.1. Simulation parameters and system set-up

The impedance mismatch between the two systems (FDTD and MD) was probed as a function of the central frequency of the wave packet (ν). Simulations were carried out for two values of ν namely 0.393 GHz and 3.93 GHz with a_0 equaling 50 Å and 5 Å, respectively. Though, the maximum displacement a_0 equals 50 Å (which is greater than the length of the FDTD element), the strain on any element is only a fraction of its length (refer equations (1)) for the definition of strain). At every frequency, the size of the FDTD time step (Δt) was systematically decreased, and the impedance mismatch was studied as a function of N_{md}, with N_{md} equaling (94, 47, 23, 12, 8, 4).

The signal is initially centred about the 5000th element and is propagated along the positive X direction. The MD cell is located at element 6000 (refer figure 2). The coupling is examined by analysing the reflected signal at an element some distance away from the MD cell. This signal is compared and contrasted with the signal that is reflected in the case when the MD cell behaves as an FDTD element with a non-linear C_{11} as determined previously from the third-order (σ) vs (ε) relationship. The latter case will be referred to as the 'pseudo MD–FDTD coupling (PC)' while the former will be referred to as 'real-time MD–FDTD coupling (RTC)'. Discrete fast Fourier transforms (FFT) [17] are used in obtaining the frequency spectrum of all the signals.

3.1.1. Case 1: ($\nu = 0.393$ GHz). Figure 3 represents the signal as it propagates (for the case when $N_{\mathrm{md}} = 94$) as well as its frequency spectrum. Even though a cursory glance at figure 3 may appear to indicate to the naked eye that the signal propagates through the medium without any loss, there is a fraction of the initial signal that is reflected from the MD–FDTD interface.

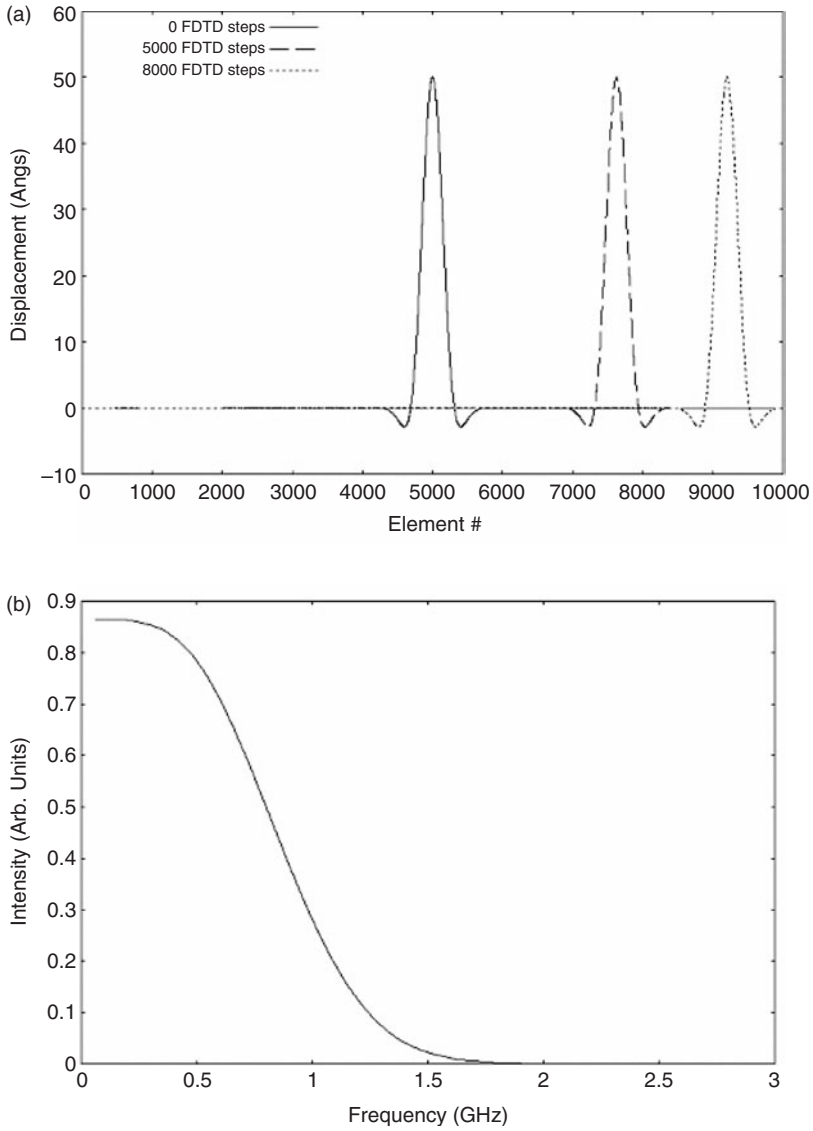

Figure 3. (*a*) Time evolution of the wave packet at 0.393 GHz for $N_{\mathrm{md}} = 94$, (*b*) frequency spectrum of the wave packet.

The reflected signals (both RTC and PC) were obtained as a function of N_{md} (figure 4). The magnitude of the reflected signals does not change significantly as a function of N_{md}. Therefore in this paper we discuss the signals for some representative cases ($N_{\mathrm{md}} = 94$, 47, 23 and 4). As obvious from figure 4, the magnitude of the 'PC' signal is always smaller than the 'RTC' signal, though the general shapes of the signals are identical.

The frequency spectra of these signals are shown in figure 5. One notices the fact that for every value of N_{md}, the lower end of the frequency spectrum for both the 'RTC' and the 'PC' signals are pretty similar, with the number of features (humps) in the signals increasing with decreasing N_{md}. In addition, for every N_{md}, the 'PC' signal has an upper cutoff at around 3 GHz, while the 'RTC' signal has a cutoff at around 150 GHz.

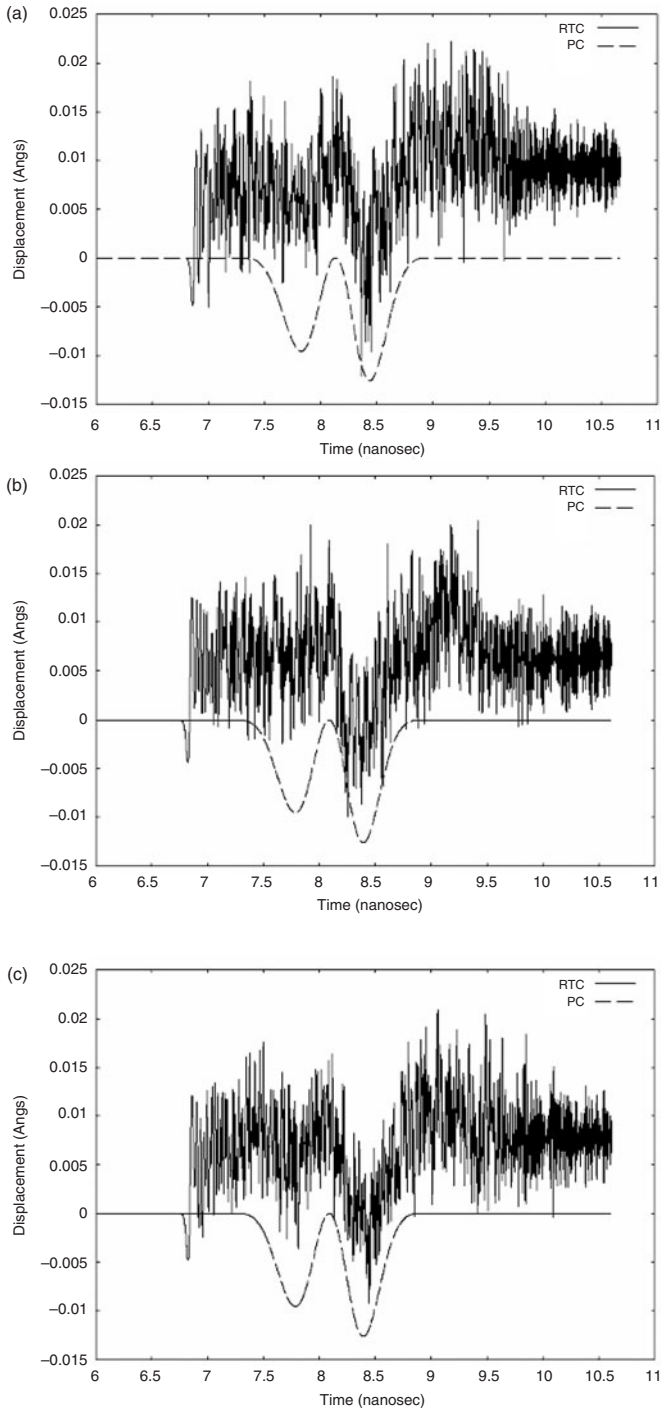

Figure 4. Amplitude of the reflected signals at 0.393 GHz when (*a*) $N_{\mathrm{md}} = 94$, (*b*) $N_{\mathrm{md}} = 47$, (*c*) $N_{\mathrm{md}} = 23$, (*d*) $N_{\mathrm{md}} = 4$.

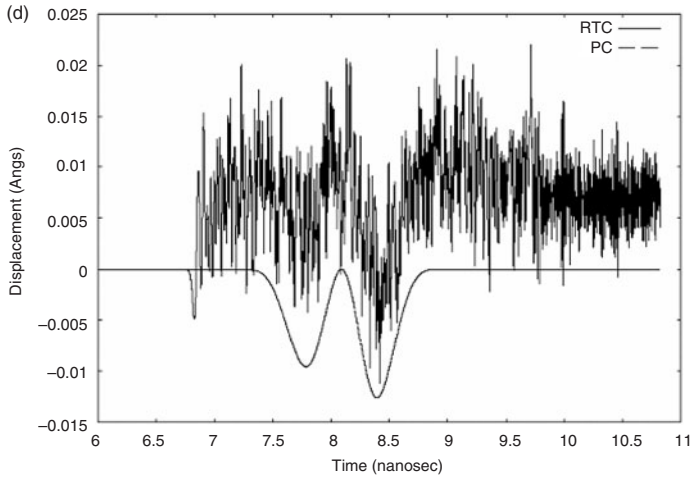

Figure 4. (Continued)

3.1.2. Case 2: ($\nu = 3.930\,GHz$). As in the previous case, though the signal appears to propagate without any visible loss (figure 6), there is a small amount of reflection. Similar to the previous case, the amount of reflection does not depend significantly on N_{md}. But unlike the previous case, the 'RTC' signals are not similar to the 'PC' signals. There is a clear mismatch in the frequency spectrum of the two signals, with the intensity of the frequencies being significantly higher for the 'RTC' signals (figure 7). The cutoff for the 'PC' signals (figure 8) is around 30 GHz, which is an order of magnitude greater than the cutoff for case 1. This corresponds exactly to the fact that ν for case 2 is an order of magnitude greater than ν for case 1. Interestingly, the cutoff for the 'RTC' signals is still around 150 GHz.

3.2. Discussion

The previous section clearly showed the following: the amount of reflection (of both RTC and PC signals) was extremely small and independent of N_{md}. The 'PC' and the 'RTC' spectra were comparable at the lower probing frequency, and the mismatch greatly increased for the higher probing frequency. The 'RTC' and the 'PC' signals had distinct cutoffs, with the cutoff for the 'PC' signals being much smaller than that of the 'RTC' signals. This can be explained on the basis that the 'PC' signal represents the long-time limit of the coupling, where the high frequency (short wavelength) modes are averaged out, while the abrupt cutoff for the 'RTC' signal represents an upper-limit in the frequencies that can be supported by the FDTD system. The discretization of the continuum into small elements modifies its dispersion relation by introducing an upper limit on the frequencies (a Debye-like frequency) that can be resolved. This upper limit on frequency for travelling waves depends on the extent of discretization of the continuum i.e. the size of the element. The effect of this frequency cutoff will be illustrated further.

3.2.1. FDTD/MD coupling with no probing signal. Consider the case of a stand-alone MD simulation at zero external pressure. The internal stress of the MD cell will typically oscillate about zero such that the average stress equals zero if the simulation is run for many MD time steps. The frequency spectrum of the stress for the model stand-alone MD system used in

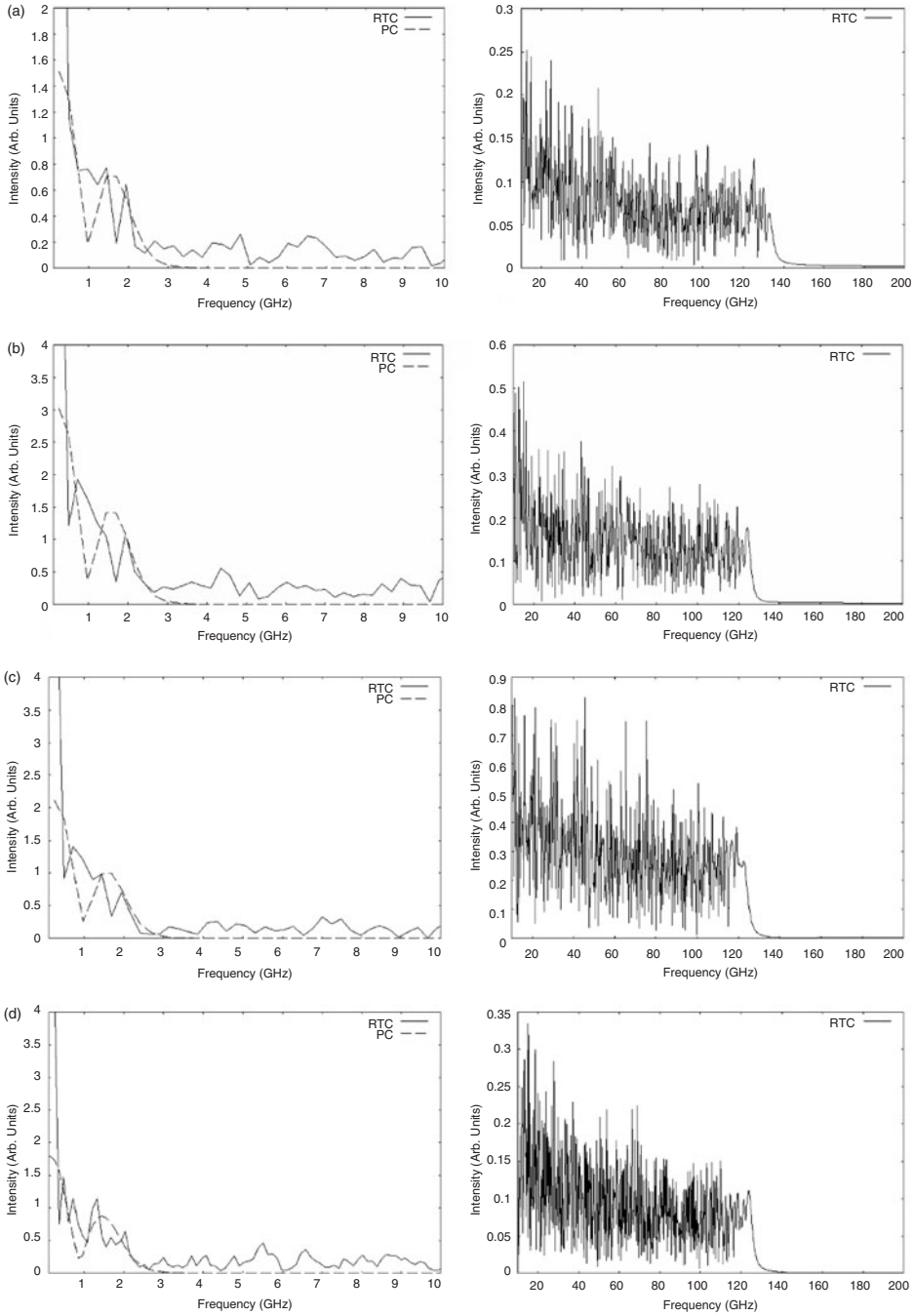

Figure 5. Frequency spectrum of the reflected signals at 0.393 GHz; (*a*) $N_{\mathrm{md}} = 94$, (*b*) $N_{\mathrm{md}} = 47$, (*c*) $N_{\mathrm{md}} = 23$, (*d*) $N_{\mathrm{md}} = 4$. For each case the figure on the left represents the low frequency range of the signal, while the figure on the right represents the high frequency range of the signal. Here 'RTC' corresponds to a real-time coupling between the FDTD and the MD region and 'PC' corresponds to a pseudo-coupling between the two regions.

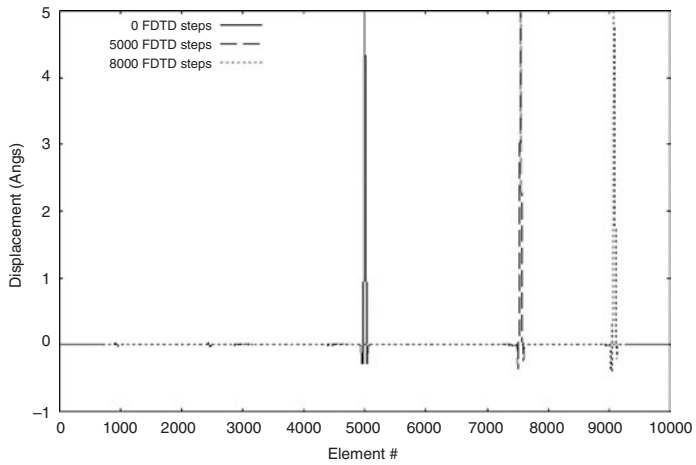

Figure 6. Time evolution of the wave packet at 3.930 GHz for $N_{\mathrm{md}} = 94$.

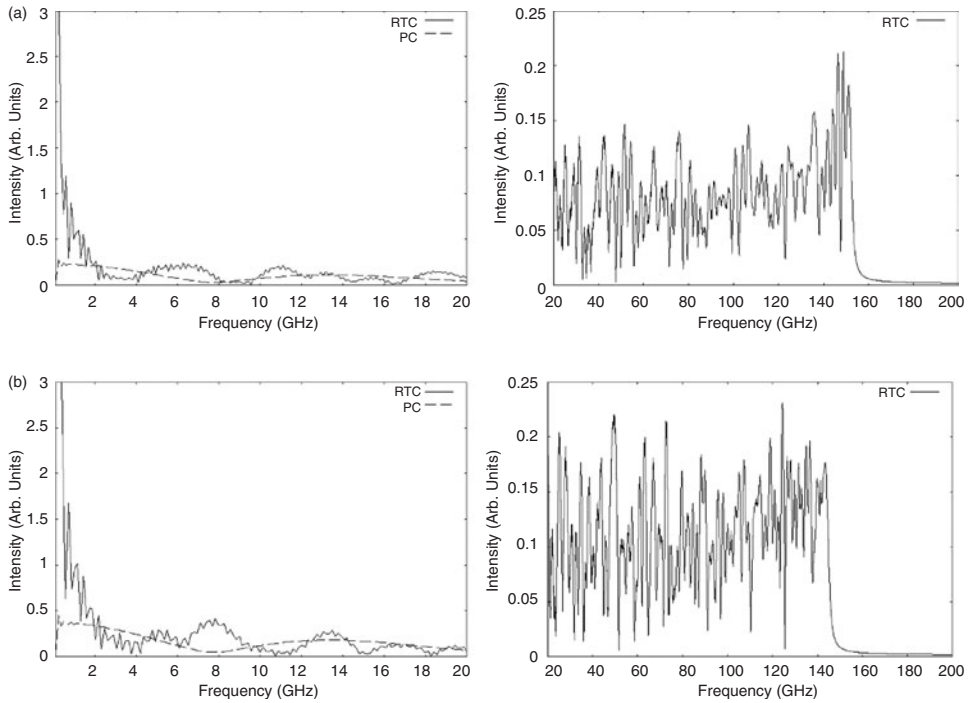

Figure 7. Frequency spectrum of the reflected signals at 3.930 GHz; (*a*) $N_{\mathrm{md}} = 94$, (*b*) $N_{\mathrm{md}} = 23$. For (*a*) and (*b*) the figure on the left represents the low frequency range of the signal, while the figure on the right represents the high frequency range of the signal. Here 'RTC' corresponds to a real-time coupling between the FDTD and the MD region and 'PC' corresponds to a pseudo-coupling between the two regions.

our simulations was determined and is shown in figure 9. The frequency spectrum of the stand-alone MD cell spans frequencies up to several 10^{12} Hz. As a next step we carried out an FDTD–MD multiscale simulation (with the same conditions used for the wave propagation studies when $N_{\mathrm{md}} = 4$), except for the fact that there was no probing wave packet. The

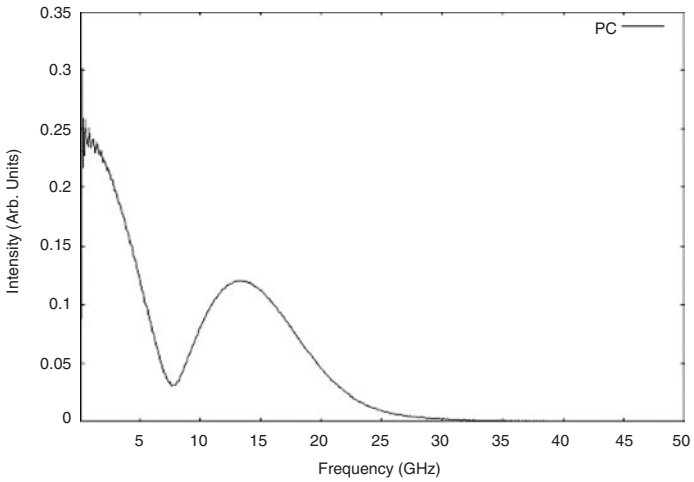

Figure 8. The complete 'PC' frequency spectrum of the reflected signal at 3.930 GHz for $N_{\mathrm{md}} = 94$. 'PC' corresponds to a PC between the FDTD and the MD regions. Since the 'PC' signals for every N_{md} are very similar, only a representative case is shown.

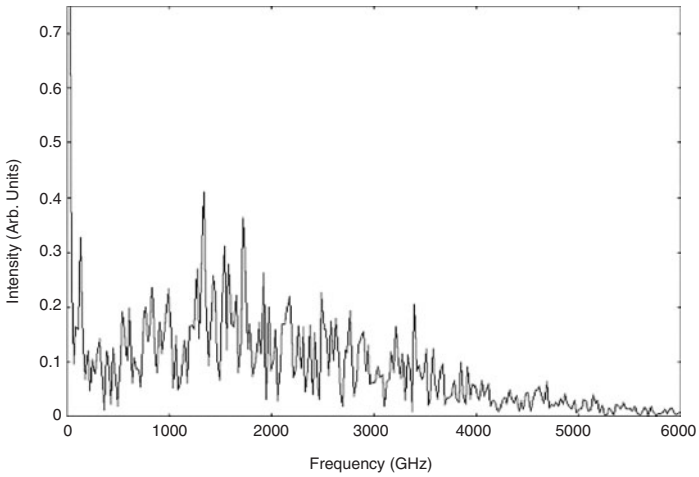

Figure 9. Frequency spectrum of the stress for the model stand-alone MD system.

frequency spectrum of the coupled MD cell was obtained and is shown in figure 10. The spectrum shows a distinct peak at 160 GHz; this mode of vibration associated with a feedback resonance between the thermalized MD and the FDTD region. This resonant mode of vibration arises because of the way the two regions are coupled (refer to the definition of strain and stress on any element in equations (1)). Here the FDTD cells neighbouring the MD cell respond to its stress fluctuation in the form of a non-zero displacement; this displacement in turn strains the MD cell with a subsequent change in internal stress. The resonant frequency is a characteristic of the size of the MD cell and corresponds to a wavelength of about 80 Å, which is about three times the size of an FDTD element. In addition, frequency spectra of the displacements of elements away from the MD cell were also obtained (figure 9). Figure 9 clearly shows the fact that as one moves away from the MD cell, the cutoff moves to lower frequencies suggesting

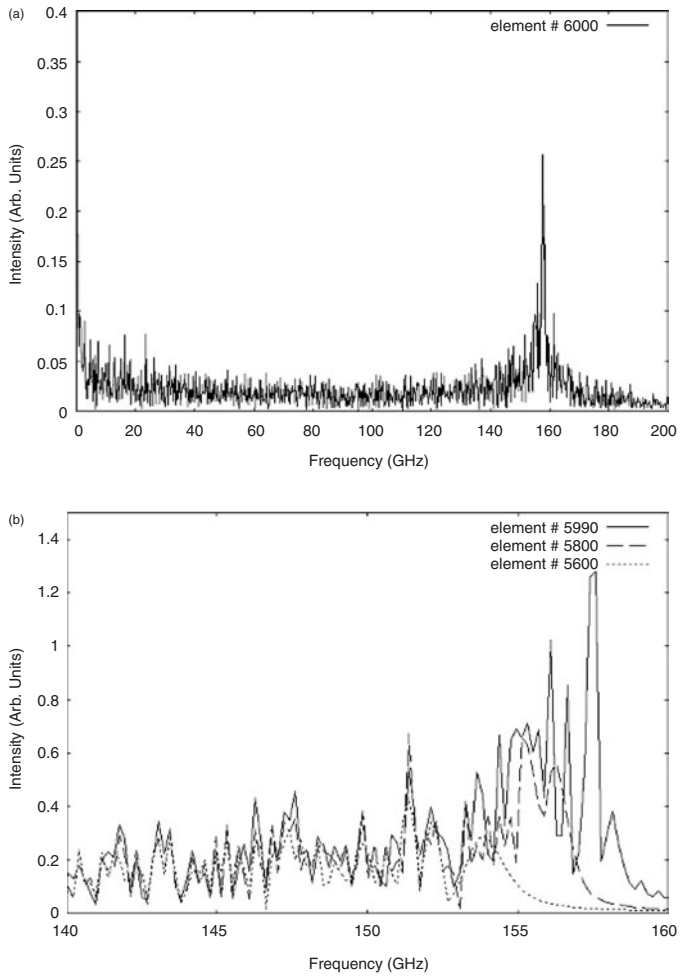

Figure 10. (*a*) Frequency spectrum of the MD cell (element 6000) when coupled with FDTD elements. (*b*) Frequency spectra of FDTD elements at various distances away from the MD cell. The inset of the respective figures refers to the location of the elements.

that the discretized FDTD system possesses a Debye-like frequency below 160 GHz. The resonant FDTD–MD vibrational mode appears therefore as a 'localized' mode in the vicinity of the MD cell, with the amplitude decaying as one moves away from the MD cell. The above fact combined with the knowledge that the MD cell transmits additional thermalized energy (corresponding to the higher frequency modes present in the RTC signals) makes the current multiscale system non-conservative. Thus defining a 'reflection coefficient' for this system becomes a difficult proposition, as in addition to the system being non-conservative, one has to separate the MD transmitted energy from the 'pure' reflected energy arising from the coupling.

4. Conclusions

The coupling between an elastic discretized continuum FDTD region and an atomistic MD region was examined by probing the MD/FDTD interface by an elastic wave with broadband

spectral features. The impedance mismatch between the two regions was studied by analysing the reflection (of the probing wave) at the interface as a function of the central frequency (ν) of the probing elastic wave under two conditions: (1) a RTC between the MD and FDTD regions (RTC); (2) the MD cell being replaced by an FDTD element such that the elastic constant of the FDTD element equals the long-time limit value. In other words, the FDTD element behaves as a pseudo MD cell (PC).

The lower end of the frequency spectrum of both the 'PC' and 'RTC' signals were similar for $\nu = 0.393\,\mathrm{GHz}$, though there was a significant mismatch when $\nu = 3.930\,\mathrm{GHz}$. The cutoffs for the RTC and the PC signals were at totally different frequencies, with the cutoff for the RTC signal corresponding to a resonant feedback mode between the FDTD and the MD regions. The extent of discretization of the continuum imposed a Debye-like limit on the frequency propagation characteristics of the discretized continuum leading to the localization of the resonant mode in the vicinity of the MD cell.

There was no significant difference in the magnitude of the reflection as the time steps of the two simulations (FDTD and MD) were pushed closer to each other (i.e. as we decrease N_{md}). However at every N_{md}, the 'PC' signal (representing the long-time limit) was significantly smaller.

Acknowledgment

This work was supported by the National Science Foundation under Grant No 9980015.

References

[1] Mullins M and Dokanish M A 1982 Simulation of the (001) plane crack in α-iron employing a new boundary scheme *Phil. Mag.* A **46** 771

[2] Tadmor E B, Phillips R and Ortiz M 1996 Mixed atomistic and continuum models of deformation in solids *Langmuir* **12** 4529

[3] Frantziskonis G and Deymier P A 2000 Wavelet methods for analyzing and bridging simulations at complementary scales—The compound wavelet matrix and application to microstructure evolution *Modelling Simul. Mater. Sci. Eng.* **8** 649–64

[4] Kitagawa H, Nakatami A and Sibutani Y 1994 Molecular dynamics study of crack process associated with dislocation nucleated at the tip *Mater. Sci. Eng.* A **176** 263

[5] Broughton J Q, Abraham F F, Bernstein N and Kaxiras E 1999 Concurrent coupling of length scales: methodology and application *Phys. Rev.* B **60** 2391

[6] Kohlhoff S, Gumbsch P and Fischmeister H F 1991 Crack-propagation in BCC crystals studied with a combined finite-element and atomistic model *Phil. Mag.* A **64** 851

[7] Abraham F F, Broughton J Q, Bernstein N and Kaxiras E 1998 Spanning the length scales in dynamic simulation *Comp. Phys.* **12** 538

[8] Ogata S, Lidorikis E, Shimojo F, Nakano A, Vasishta P and Kalia R K 2001 Hybrid finite element/molecular dynamics/electron density functional approach to materials simulations on parallel computers *Comp. Phys. Comm.* **138** 143

[9] Shenoy V B, Miller R, Tadmor E B, Rodney D, Phillips R and Ortiz M 1999 An adaptive finite element approach to atomic-scale mechanics—the quasicontinuum method *J. Mech. Phys. Solids* **47** 611

[10] Rudd R E and Broughton J Q 1998 Coarse-grained molecular dynamics and the atomic limit of finite elements *Phys. Rev.* B **58** R5893

[11] Kittel C 1976 *Introduction to Solid State Physics* 5th edn (New York: Wiley) p 111

[12] Sigalas M M and Garcia N 2000 Theoretical study of three dimensional elastic band gaps with the finite difference time domain method *J. Appl. Phys.* **87** 32122

[13] Garcia-Pablos D, Sigilas M M, de Espinosa F R M, Torres M, Kafesaki M and Garcia N 2000 Theory and experiments on elastic band gaps *Phys. Rev. Lett.* **84** 4339

[14] Rapaport D C 1995 *The Art of Molecular Dynamics Simulation* (Cambridge: Cambridge University Press)

[15] Parrinello M and Rahman A 1981 Polymorphic transitions in single crystals—A new molecular dynamics method *J. Appl. Phys.* **52** 7182
[16] Garcia A L, Bell J B, Crutchfield W Y and Alder B L 1999 Adaptive mesh and algorithm refinement using direct simulation Monte Carlo *J. Comp. Phys.* **154** 134
[17] Press W H, Teulosky S A, Vetterling W T and Flannery B P 1992 *Numerical recipes in Fortran, The Art of Scientific Computing* 2nd edn (Cambridge: Cambridge University Press) pp 501–2